

# Quantification of chaotic dynamics for heavy particle dispersion in ABC flow

Lian-Ping Wang,<sup>a)</sup> Thomas D. Burton, and David E. Stock  
*Department of Mechanical and Materials Engineering, Washington State University, Pullman,  
Washington 99164-2920*

(Received 28 August 1990; accepted 27 December 1990)

A six-dimensional nonlinear dynamic system describing the Lagrangian motion of a heavy particle in the Arnold–Beltrami–Childress (ABC) flow was numerically studied. Lyapunov exponents and fractal dimension were used to quantify the chaotic motion. A single set of ABC flow parameters and a limited set of initial conditions were used. Given these restrictions, the following were found. (1) Attractor fractal dimension varies significantly with Stokes number, and, depending on inertia, periodic, quasiperiodic, and chaotic attractors may exist. (2) Particle drift reduces the fractal dimension when the drift is small. It can also cause irregular jumps when the drift parameter is close to one. (3) Quasiperiodic orbits on smooth two-dimensional manifolds were shown to be the most common ultimate solutions of the system when either the inertia or the drift is relatively large. (4) Different initial conditions can lead to different attracting sets; however, most of them have the same dimension. (5) A direct measure of dispersion based on mean square displacement was defined, but no relation between this dispersion measure and fractal dimension was found.

## I. INTRODUCTION

Mixing, diffusion, and dispersion of passive particles in a fluid flow are naturally related to the particle's motion along its trajectory,<sup>1</sup> i.e., the Lagrangian motion, as opposed to the Eulerian motion based on fixed space coordinates. If the Eulerian flow field is known, the Lagrangian motion is then defined by a set of nonlinear ordinary differential equations, usually a dynamical system rich enough to display nonintegrable or chaotic behavior. Recently, the methods of modern nonlinear dynamics have been used to study the Lagrangian motion of particles and fluid points.<sup>2–6</sup> Even in simple steady flows, such as the Stokes flow or the Arnold–Beltrami–Childress (ABC) flow, the Lagrangian motion of fluid particles can be chaotic.<sup>2,3</sup> Aref and Jones<sup>6</sup> found that, if the flow exhibited chaotic advection, separation of diffusing fluid particles in a Stokes flow was enhanced.

In this paper, we consider the motion of heavy particles under linear Stokes drag in the ABC flow. Heavy particles are any small passive particles in the flow with a density much larger than the density of the fluid. In an external potential force (usually gravity) field, heavy particles have a free-fall velocity that is of the order of the fluid characteristic velocity. The density difference and free fall cause the heavy particle to not exactly follow the motion of the surrounding fluid. The equations of motion for a heavy particle can be written in dimensionless form as

$$\frac{dv_i}{dt} = \frac{u_i(\mathbf{y}, t) - v_i}{St} - \frac{\gamma \delta_{i3}}{St}, \quad i = 1, 2, 3; \quad (1a)$$

$$\frac{dy_i}{dt} = v_i, \quad i = 1, 2, 3. \quad (1b)$$

Here, Stokes number,  $St \equiv \tau_a u_0 / L$ , is the ratio of a particle's aerodynamic response time to a characteristic time of the

flow,  $\gamma = \tau_a g / u_0$  is the ratio of the particle's drift velocity  $\tau_a g$  to a characteristic velocity of the flow, where  $L$  and  $u_0$  are the characteristic length and velocity of the flow, respectively, and  $g$  is the body force per unit mass, and  $u_i(\mathbf{x}, t)$  represents the instantaneous Eulerian fluid velocity. For steady ABC flow, the flow field is defined by

$$u_1 = A \sin(2\pi x_3) + C \cos(2\pi x_2), \quad (2a)$$

$$u_2 = B \sin(2\pi x_1) + A \cos(2\pi x_3), \quad (2b)$$

$$u_3 = C \sin(2\pi x_2) + B \cos(2\pi x_1). \quad (2c)$$

This flow is an exact solution of Euler's equation, because the vorticity vector is parallel to the velocity vector at all points in space. In the real world, this flow would decay because of the viscosity of the fluid. The details of the flow structure have been discussed by Dombre *et al.*<sup>3</sup>

The dynamical system (1a) and (1b) is six-dimensional, strongly nonlinear, and nonautonomous. It is dissipative, since the volume expansion rate associated with (1a) and (1b) is  $-3/St$  if the flow is incompressible. It is also quite different from the dynamic system for the motion of fluid points, Eq. (1b) with  $v_i$  replaced by  $u_i$ , which is three-dimensional and nondissipative. The chaotic motion of passive particles in this ABC flow was investigated by McLaughlin.<sup>5</sup> He found that chaotic particle trajectories existed and that chaos tended to be eliminated by the particle inertia and virtual mass. McLaughlin did not quantify the chaotic behavior. In addition, he reduced the six-dimensional dynamic system to a three-dimensional dynamic system by assuming the inertia to be small. In his study, the particle velocity  $v_i(t)$  was given simply by replacing  $dv_i/dt$  in Eq. (1a) with  $du_i/dt$ . Therefore his dynamic system for the motion of particles is valid only when the inertia is very small (i.e.,  $St \ll 1$ ).

Most of the work on the chaotic dynamics of Lagrangian motion is still in its qualitative stage. In our recent paper (Wang *et al.*<sup>7</sup>), we calculated quantitative measures of both dispersion and chaos and found that the dispersion coefficient of heavy particles in pseudoturbulence is linearly relat-

<sup>a)</sup> Present address: Center for Fluid Mechanics, Turbulence, and Computation, Box 1966, Brown University, Providence, Rhode Island 02912. (Visiting Research Associate.)

ed to the fractal dimension of the attractor for the heavy particles. In this paper, we shall examine quantitatively the Lagrangian motion of heavy particles in the ABC flow in terms of both dispersion and chaotic behavior. ABC flow is very different than pseudoturbulence. The latter is random, statistically isotropic, and homogeneous. ABC flow, on the other hand, is spatially periodic, well organized, anisotropic, and inhomogeneous. Crisanti *et al.*<sup>8</sup> quantitatively studied the Lagrangian motion of particles in a two-dimensional counterpart of the ABC flow with  $A = B = 2$  and  $C = 0$ . For particles slightly heavier than the fluid, they found that the particle motion can be characterized by well-defined dispersion coefficients and a positive largest Lyapunov exponent. They also showed, through numerical simulations, a similarity between the particle motion and the motion of fluid elements in the presence of molecular diffusion. Because of the recent finding of *Lagrangian turbulence*,<sup>2-6</sup> we believe that a dispersion measure makes sense when the particle motion becomes chaotic, even the flow responsible for such motion is simple and steady. If the particle motion happens to be periodic or quasiperiodic, the dispersion measure is not a valid notion. Indeed the possible breakdown of the dispersion measure here motivates us to search for a better way of quantifying the Lagrangian particle motion, i.e., to use fractal dimension.

The purpose of this study was to numerically calculate both fractal dimension and a measure of dispersion for the Lagrangian motion of heavy particles in ABC flow. The six-dimensional nonlinear ODE, (1a) and (1b), were used since both finite inertia and finite drift were considered. Lyapunov exponents were used to estimate the fractal dimension (Kaplan–Yorke conjecture<sup>9</sup>). Time-averaged mean square displacements were introduced to quantify the dispersion.

In this paper, we will describe only some preliminary results of our study. The complexities contained in the system are illustrated through a limited choice of the system parameters and the initial conditions. A more detailed study is currently in progress.

## II. COMPUTATION DETAILS AND FRACTAL DIMENSION

Since the dynamic system, (1a) and (1b), is generally nonintegrable, numerical integration is necessary to determine the Lagrangian motion. This was done using the fourth-order Hamming<sup>10</sup> predictor–corrector scheme, with initialization using the fourth-order Runge–Kutta method. A time step of 0.01 was used in this study. Numerical tests showed that the Poincaré map and Lyapunov exponents were independent of time step for time steps smaller than 0.01.

In this study, we focused on how the Lagrangian motion of a heavy particle would change with particle's characteristics, the Stokes number, and the drift parameter. One set of flow parameters,  $A = 1$ ,  $B^2 = 0.9$ ,  $C^2 = 0.5$ , was used. For this set of  $A$ ,  $B$ , and  $C$  values, we have  $B^2 + C^2 > A^2$ . It is known that there are eight distinct fixed points in the fundamental box  $0 < x < 1$ ,  $0 < y < 1$ ,  $0 < z < 1$  and that regions of chaos exist along the heteroclinic lines connecting the unstable fixed points for the Lagrangian motion of fluid elements<sup>2</sup>

(note: if the drift is zero, the fixed points for the motion of heavy particle are exactly the same as those of fluid elements).

The initial conditions for the motion of a heavy particle were taken to be

$$y_i(t=0) = y_{0i}, \quad (3a)$$

$$v_i(t=0) = u_i(y_{0i}, 0) - \gamma \delta_{i3}. \quad (3b)$$

The value for the initial location,  $y_{0i}$  in (3a), may affect the long-time solution of the Lagrangian motion. To test this, we used two different initial locations,  $S_1$ : (0.26, 0.0, 0.5) and  $S_2$ : (0.3, 0.1, 0.6) in our calculations. The point  $S_1$  is near the edge of one of the principal vortices<sup>2</sup> aligned along with the  $x_1$  direction. The point  $S_2$  is close to one of the fixed points (0.328, 0.109, 0.592). Other initial locations will be discussed later in the paper.

The initial particle velocity may not be realistic. We chose (3b) mainly for the purpose of limiting the number of conditions to be studied. If the long-time solution of the system is not unique, different choices of initial conditions may lead to different attractors. See Sec. IV C for a limited discussion of the effect of initial conditions on the type of attractor realized.

Lyapunov exponents characterize the mean exponential rate of divergence of trajectories surrounding a given trajectory in a phase space. For the autonomous six-dimensional system given by (1a) and (1b), there exist six Lyapunov exponents.<sup>11</sup> It is well known that a dissipative nonlinear system may have a variety of different attracting sets for different system parameters and initial conditions,<sup>12</sup> therefore the Lyapunov exponents are not unique. In this study, the Lyapunov exponents were found using the procedure of Wolf *et al.*<sup>13</sup> A brief description of the procedure is given here. A base trajectory was produced first by numerical integration of the motion equations of a particle. Then, six neighboring trajectories were computed using the linearized version of the equations of motion, starting from six orthonormal directions. A Gram–Schmidt reorthonormalization procedure on the vector frame was used after every time duration  $\tau$  to form a new orthonormal set. After  $n$  intervals, the Lyapunov exponents were estimated by

$$\sigma_i(n) = \frac{1}{n\tau} \sum_{j=1}^n \log_2 [\text{Norm}_i(j)], \quad i = 1, \dots, 6, \quad (4)$$

where  $\text{Norm}_i(j)$  is the length of projection of the evolved vector  $i$  in its new normalization direction at time  $j\tau$ . If  $n$  is sufficiently large,  $\sigma_i$  will no longer depend on  $n$  (Fig. 1). For most of the results presented,  $n$  is 4000 and  $\tau$  is 1.0. Two important features of the Lyapunov exponents were observed in our computations: (1) At least one of the Lyapunov exponents was zero (all of the attractors we found were of dimension of one or greater); (2) the sum of the Lyapunov exponents was equal to  $-3/\text{St}$  multiplied by the factor  $\log_2 e$ .

A further measure of a system attractor is the fractal dimension. The Kaplan and Yorke or Lyapunov dimension<sup>9,13</sup>  $d_f$  was calculated as

$$d_f = j + \frac{\sum_{i=1}^j \sigma_i}{|\sigma_{j+1}|}, \quad (5)$$

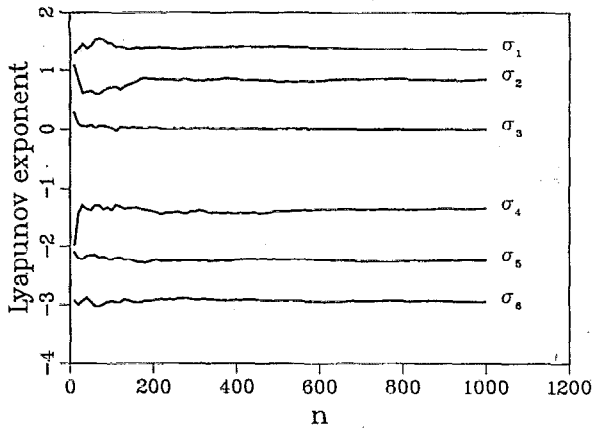


FIG. 1. Lyapunov exponents as a function of the number of intervals for the attractor of Lagrangian motion of a heavy particle starting from the point  $S_1$  and with  $St = 1.0$  and  $\gamma = 0.0$ .

where  $j$  is defined by the condition that

$$\sum_{i=1}^j \sigma_i > 0 \quad \text{and} \quad \sum_{i=1}^{j+1} \sigma_i < 0. \quad (6)$$

### III. MEASURE OF DISPERSION

One measure of the dispersion of particles in a turbulent flow is diffusivity, which is one-half of the time derivative of mean square displacement. For homogeneous flows, the long-time mean square displacement is a linear function of time and thus it is possible to calculate a long-time diffusivity. This idea was used to introduce a measure of dispersion for the motion of particles in our deterministic and steady ABC flow. The use of a dispersion measure here was motivated by the recent finding of *Lagrangian turbulence*<sup>2-6</sup> and the practical relevance of quantifying Lagrangian motions.

The mean square displacement was calculated from one trajectory of a heavy particle. We divided the trajectory into  $N$  sections of time length  $T_0$ . For each section, we defined the displacement  $\hat{y}_i(t, k)$  as the change of location relative to the starting point of the section,  $\hat{y}_i(t, k) = y_i[(k-1)T_0 + t] - y_i[(k-1)T_0]$ . Then the mean square displacement is

$$\overline{\Delta \hat{y}_i^2(t)} = \frac{1}{N} \sum_{k=1}^N [\hat{y}_i(t, k) - \overline{\hat{y}_i(t)}]^2, \quad \text{for } 0 \leq t < T_0, \quad i = 1, 2, 3, \quad (7a)$$

where the mean displacement is defined as

$$\overline{\hat{y}_i(t)} = \frac{1}{N} \sum_{k=1}^N \hat{y}_i(t, k). \quad (7b)$$

The *mean diffusivity*  $\bar{\epsilon}(t)$  is one-half of the time derivative of the average mean square displacement

$$\bar{\epsilon}(t) = \frac{1}{6} \frac{d}{dt} [\overline{\Delta \hat{y}_1^2(t)} + \overline{\Delta \hat{y}_2^2(t)} + \overline{\Delta \hat{y}_3^2(t)}]. \quad (8)$$

A constant long-time diffusivity can be calculated if the average mean square displacement is linearly related to  $t$  when  $t$  is sufficiently large. Figure 2 shows the mean square displacements for two different  $\gamma$  with  $St = 1$ . At  $\gamma = 0.0$ , the average long-time mean square displacement is a linear func-

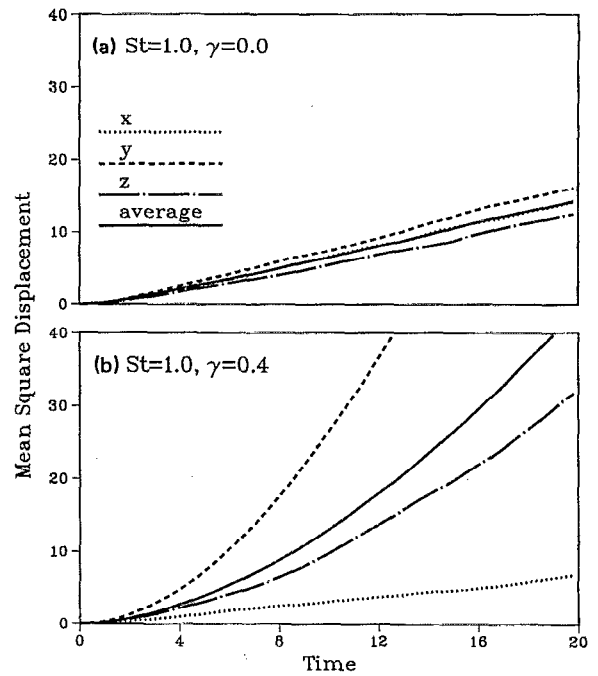


FIG. 2. Mean square displacements for a heavy particle starting from  $S_1$  and with  $St = 1.0$ . A long-time diffusivity for  $\gamma = 0.0$  can be defined while it cannot be defined for  $\gamma = 0.4$ .

tion of time and  $\bar{\epsilon}$  is equal to 0.375. For  $\gamma = 0.4$ , the average long-time mean square displacement is not a linear function of time but is approximately proportional to  $t^2$ . Such a *ballistic* dispersion was also observed by Crisanti *et al.*<sup>8</sup> For this case, the long-time diffusivity cannot be defined. Direct visualization (three-dimensional trajectory plots) indicated that the trajectory for  $\gamma = 0.0$  and  $St = 1.0$  has a very irregular shape, while the trajectory for  $\gamma = 0.4$  and  $St = 1.0$  is quasi-periodic with a helical turning behavior. We will report the value of the long-time diffusivity only when it is defined. For all the diffusivity calculations, an  $N$  of 300 and  $T_0$  of 20 was used.

### IV. RESULTS AND DISCUSSIONS

#### A. Lagrangian motion of heavy particles with zero drift

We first consider the Lagrangian motion of a heavy particle assuming the drift is zero ( $\gamma = 0$ ). Figure 3 shows the largest Lyapunov exponent  $\sigma_1$  as a function of the Stokes number. Here,  $\sigma_1$  increases with particle inertia very rapidly for  $St < 0.3$  but decreases with particle inertia for  $0.3 < St < 2$ , and reaches its maximum value of about 2 when  $St = 0.3$ . When the Stokes number is larger than 2.25,  $\sigma_1$  is consistently close to zero. Since a positive  $\sigma_1$  is a necessary condition for chaotic motion, the Lagrangian motion of a heavy particle with large inertia is at most weakly chaotic. It is worth noting that the largest Lyapunov exponent for the attractor of a fluid element starting from  $S_1$  is 0.000, which is expected, since  $S_1$  is near one of the principal vortices and the orbit is quasiperiodic. The motion of a fluid element starting from  $S_2$  has a chaotic trajectory with  $\sigma_1$  equal to 0.517. Therefore  $\sigma_1$  for the attractor of a fluid element depends on the initial location. However,  $\sigma_1$  showed no signifi-

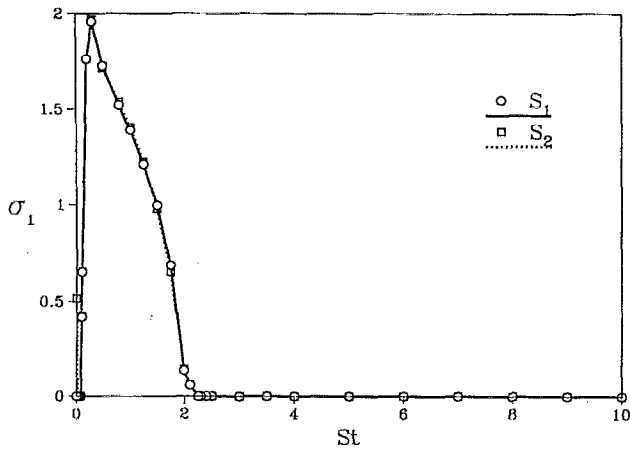


FIG. 3. Largest Lyapunov exponents as a function of the Stokes number when the drift is zero.

cant dependence on initial location for the attractor of a heavy particle for most inertia values. For a heavy particle with very small inertia and starting from  $S_2$ ,  $\sigma_1$  was near zero and thus is different than  $\sigma_1$  for a fluid element starting from the same location. This agrees with McLaughlin's qualitative result.<sup>5</sup>

The Kaplan–Yorke fractal dimension has a shape similar to  $\sigma_1$  (Fig. 4). The maximum  $d_f$  is 4.45 and occurs when  $St$  is 1.25. A Stokes number close to one is physically important since, in this case, the particle response time is about the same as the flow characteristic time. The power spectra for the three velocity components at  $St = 1.0$  are shown in Fig. 5(a). We see that the three spectrum curves are very similar and contain broadband frequency contributions, which implies that the Lagrangian particle motion is nearly random and isotropic. It is also interesting to note that the curves are almost a straight line on the log-linear plot. The  $d_f$  value for the attractor of the particle starting from  $S_1$  is very close to that starting from  $S_2$  for all  $St$ , indicating no detectable dependence of  $d_f$  on the initial location of the particle. For  $St \geq 2.25$ , the first two Lyapunov exponents are equal to zero

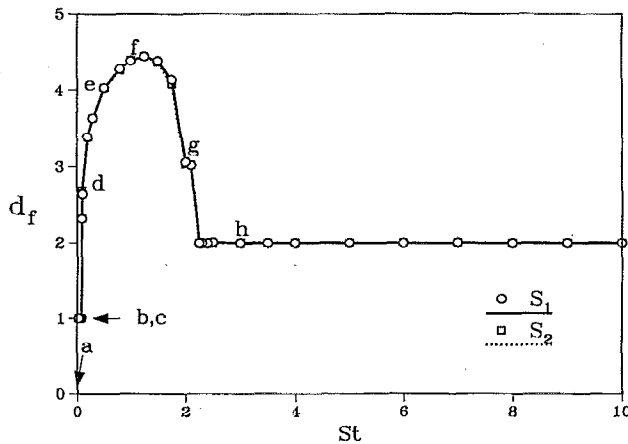


FIG. 4. Fractal dimension as a function of the Stokes number when the drift is zero.

and the remaining four less than zero so that  $d_f$  is equal to two. The velocity power spectra for such a case are shown in Fig. 5(b). All the peaks in Fig. 5(b) are resolved by using two discrete frequencies,  $f_1 \approx 3.01$  and  $f_2 \approx 3.83$ , and their combination frequencies. The fact that  $d_f = 2$  suggests that the ratio of these two frequencies is an irrational number and the motion is quasiperiodic. The attracting set for this case in the phase space is then a two-dimensional smooth manifold such as toroidal surface or closed sheet.

To gain a further understanding of the above results, we constructed Poincaré maps in the plane  $x = 0$  for the particle's orbit for some of the inertia values (Fig. 6). The Poincaré map was formed by recording the particle's  $y$  and  $z$  coordinates each time the particle crossed the plane  $x = 0$  and imposing periodic boundary conditions in all three directions.<sup>5</sup> In general, the larger the fractal dimension the more the attractor spreads on the Poincaré map. When the Stokes number is one and  $d_f$  is nearly maximized, the Poincaré map has almost a uniform distribution of intersection points and shows no structure.

Figure 7 shows the mean long-time diffusivity as a function of Stokes number. The diffusivity increases with  $St$  for  $St < 1.3$  and is very close to zero for  $St > 2.3$ . The long-time mean square displacement was not linearly related to time for  $1.3 < St < 2.3$ , thus the diffusivity could not be defined in this region. Comparing Fig. 7 to Fig. 4, we find no correlation between  $d_f$  and  $\bar{\epsilon}$ .

### B. Lagrangian motion with a fixed particle inertia ( $St = 1$ )

To study the effect of particle drift on the Lagrangian motion of a heavy particle, we now fix the particle inertia,

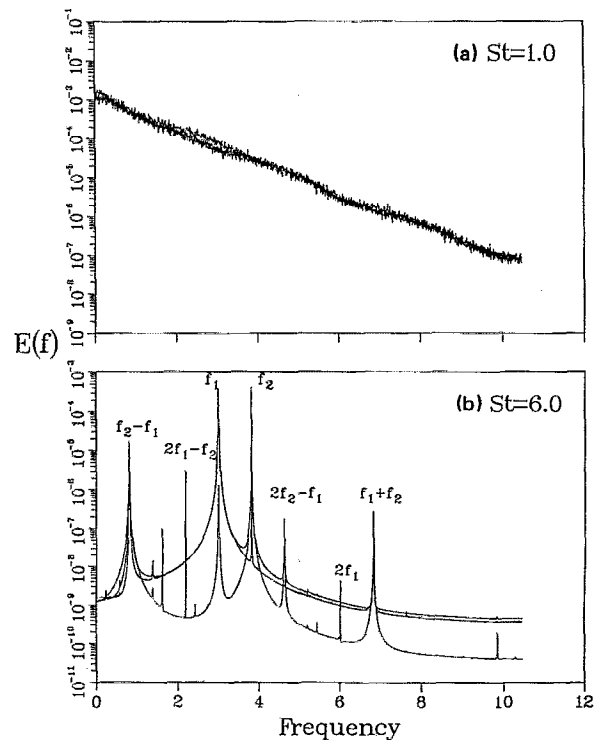


FIG. 5. Power spectra of the particle velocities  $v_i(t)$  for  $\gamma = 0$ .

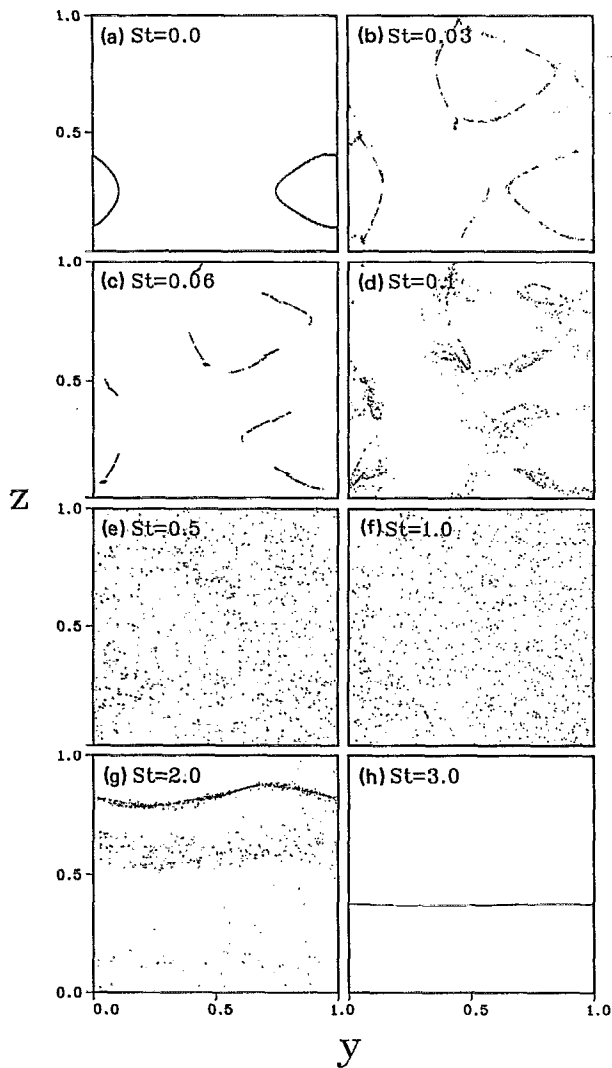


FIG. 6. Poincaré maps for some of the points shown in Fig. 4.

$St = 1.0$ . Figure 8 shows the largest Lyapunov exponent  $\sigma_1$  as a function of the drift parameter. For very small  $\gamma$ ,  $\sigma_1$  is almost constant. Then it decreases quickly with increasing  $\gamma$  for  $0.3 < \gamma < 0.5$ . For  $\gamma > 1.1$ ,  $\sigma_1$  is equal to zero, indicating

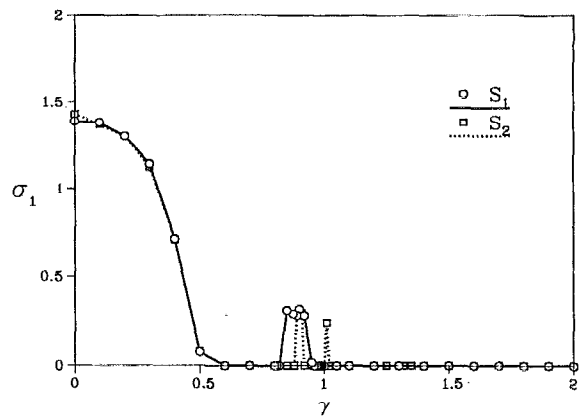


FIG. 8. Largest Lyapunov exponents as a function of the drift parameter when the Stokes number is set to one.

the motion is not chaotic. However, for the region  $0.7 < \gamma < 1.1$ , there are some irregular jumps in the value of  $\sigma_1$ . This suggests the possibility of bifurcations. The fractal dimension (Fig. 9) has a shape similar to  $\sigma_1$ . Here,  $d_f$  for  $\gamma \geq 1.2$ , as in the case of large  $St$  in Fig. 4, is equal to two, which indicates the attractor is a two-dimensional manifold. Power spectra and direct trajectory projection of the motion of a particle starting from  $S_1$  with  $\gamma = 1.7$  showed the trajectory to have a periodic orbit on a toroidal surface, i.e., two rationally related basic frequencies governing the motion. An expansion of the fractal dimension for  $0.6 < \gamma < 1.1$  is given in Fig. 10. The jumps in  $d_f$  in Fig. 10 have different shapes for different initial particle locations. Therefore, in addition to structure bifurcation, multiattractors can be present in this region. At some values of  $\gamma$ ,  $d_f$  is equal to one. Most of the  $d_f = 1$  cases can be shown to have periodic orbits on a toroidal surface, as for  $\gamma = 1.7$ . We also found that for at least one case,  $\gamma = 1.1$  and initial location  $S_1$ , the velocity power spectra show peaks at a single frequency and its multiples and the attractor projected onto the  $v_1, v_2, v_3$  space is a closed curve. These results indicate that the attractor is a limit cycle. The existence of limit cycles, quasiperiodic orbits and chaotic attractors suggest that the route to chaos for the system is via quasiperiodicity.<sup>12</sup> Further study, however, is

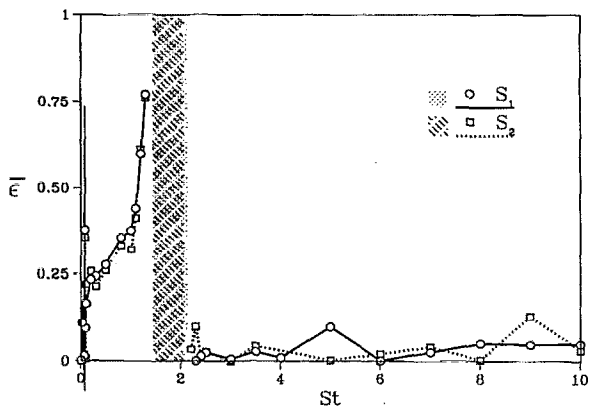


FIG. 7. Mean long-time diffusivity as a function of the Stokes number when the drift is zero. The shaded region is where the diffusivity cannot be defined.

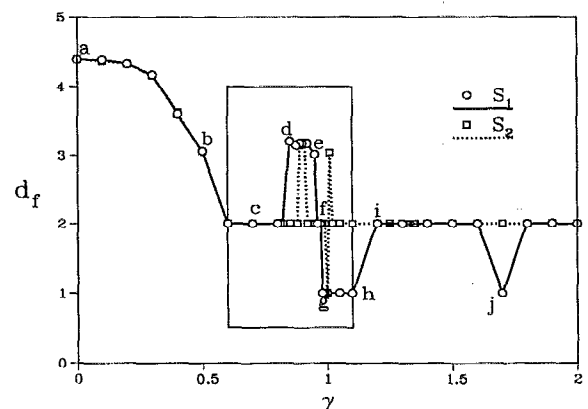


FIG. 9. Fractal dimension as a function of the drift parameter when the Stokes number is fixed to one.

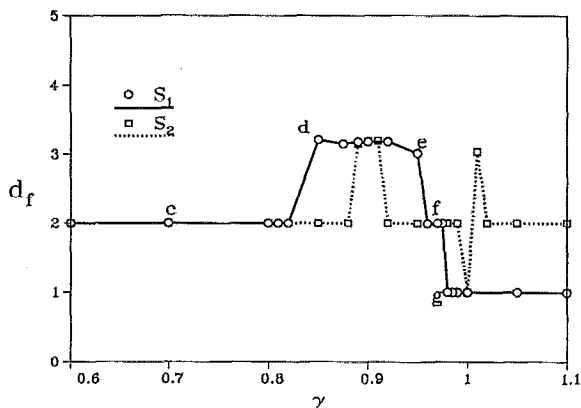


FIG. 10. An expanded view of the region from  $\gamma = 0.6$  to  $\gamma = 1.1$  in Fig. 8.

needed to verify the nature of these bifurcations. A detailed look at the Poincaré maps on the  $z = 0$  plane (Fig. 11) also suggests that the larger the fractal dimension, the more the attractor spreads on the Poincaré map.

Finally, the diffusivity for large values of  $\gamma$  ( $\gamma > 0.7$ ) is close to zero (Fig. 12). For very small values of  $\gamma$ , the diffusivity increases with the drift. For some values of  $\gamma$ , the diffusivity cannot be defined. No rational connection between  $d_f$  and  $\bar{\epsilon}$  can be drawn.

### C. Other initial conditions

A brief discussion on the effect of initial conditions on the types of attractors is given here. The nonlinear system is dissipative and it is not difficult to show that the particle velocities are bounded. The particle locations are not necessarily bounded, however, they can be truncated to the unit cubic box due to the periodicity of the ABC flow. Then, for the six-dimensional, volume-contracting and bounded system, the orbits may be asymptotic to one of the following attracting sets:<sup>14</sup> (i) stable fixed points, (ii) simple closed curves, i.e., stable limit cycles, (iii) quasiperiodic (or periodic) orbits on a two-dimensional torus (or one-dimensional toroidal curve), (iv) possible additional periodic and quasiperiodic orbits on higher dimensional surfaces, and (v) strange attractors. We can show that, for  $\gamma < \sqrt{2(C^2 + B^2 - A^2)}$ , all the fixed points of the system are unstable and, for  $\gamma > \sqrt{2(C^2 + B^2 - A^2)}$ , no fixed point exist, therefore (i) is not possible. We have observed (ii), (iii), and (v) for the limited values of particle drift and inertia and one set of  $A$ ,  $B$ , and  $C$ .

In addition, the asymptotic solution may depend on the initial conditions. A complete search of different attracting sets and their respective basins of attraction is beyond the scope of this paper and may well be impossible in practice. (For a much simpler, low-dimension system such as a nonlinear Duffing oscillator, a search of all attractors and their basins of attraction is possible but very tedious.<sup>12</sup>) Nevertheless, we have tested some other initial conditions for the following two cases: (i)  $St = 2.4$  and  $\gamma = 0$ ; (ii)  $St = 1.0$  and  $\gamma = 0.85$ . In addition to the two initial locations  $S_1$  and  $S_2$ , the computation for  $\sigma_i$  and  $d_f$  were repeated for 27 initial

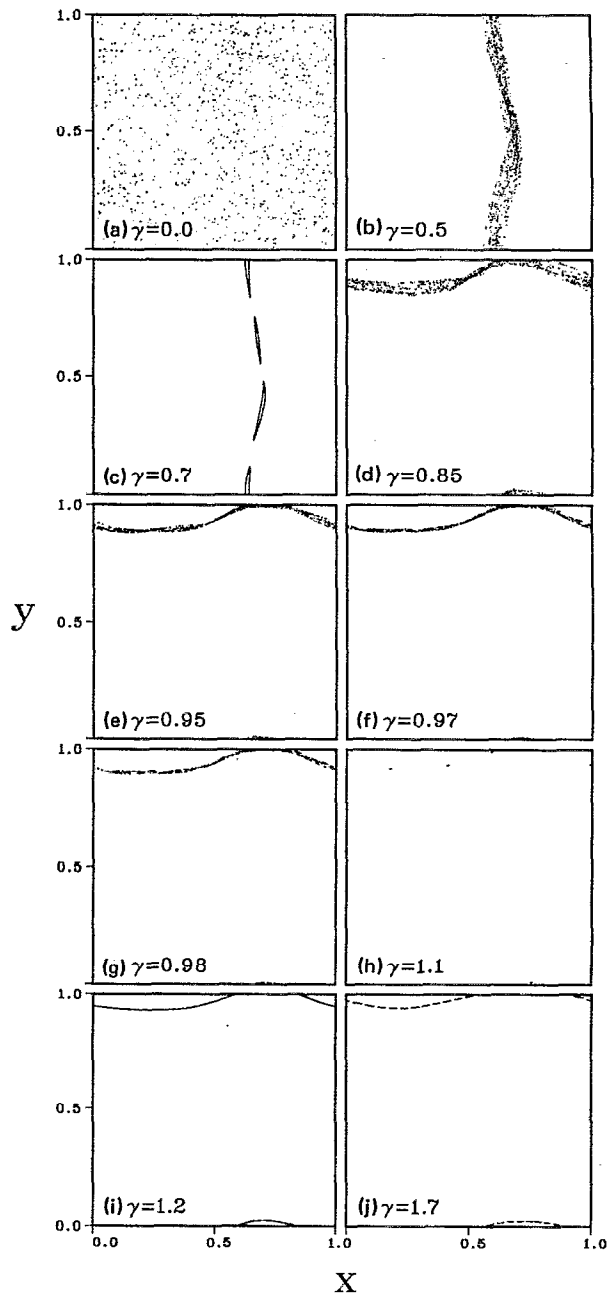


FIG. 11. Poincaré maps for some of the points shown in Figs. 8 and 9.

locations uniformly distributed in the unit cubic box, i.e.,  $x_i = \frac{1}{3}, \frac{2}{3}$ , and  $\frac{2}{3}$  for  $i = 1, 2, 3$ . The initial condition for particle velocity was still given by (3b).

For the first case, we found that no matter where the initial particle location was, the Lyapunov exponents were about the same. The first two exponents were zero and the remaining four were less than zero, leading to  $d_f = 2$ . However, the attractors were observed not to have identical structure. The solutions for all 29 initial conditions were projected onto the  $v_1 - v_2$  plane. Four solutions that have apparently different structures are shown in Fig. 13. What is not shown in the figure is the additional fact that three of the attracting sets 13(a), 13(c), and 13(d) have more than one orienta-

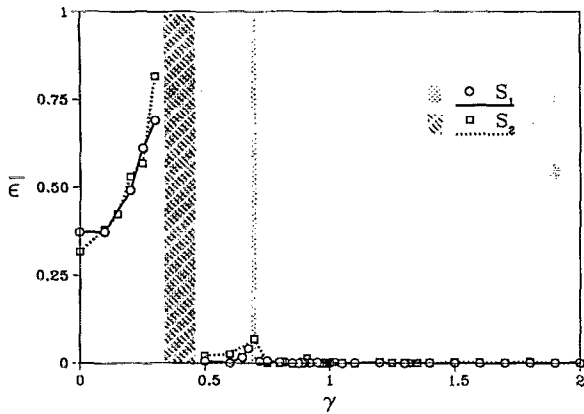


FIG. 12. Mean long-time diffusivity as a function of the drift parameter when the Stokes number is one. The shaded region is where the diffusivity cannot be defined.

tion. Four different orientations were observed for both 13(a) and 13(c). Three different orientations were seen for 13(c). This type of structure reflects the symmetry of the system. In summary, numerical solutions reveal that there are at least 12 different attractors (counting both structure and orientation differences) for the 29 initial conditions tested. (Strictly speaking, the same structure and orientation in the  $v_1$ - $v_2$  plane do not guarantee a single attractor.) Interestingly, they all have similar Lyapunov spectra and the same dimension.

For the second case, two different attracting sets of different structure and different dimension are observed (Fig. 14). Two different orientations were seen for each of the sets. Therefore we have at least four different attractors for the 29 initial conditions.

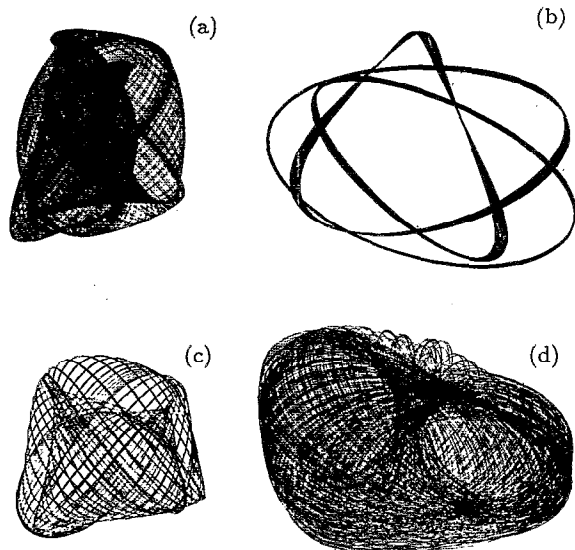
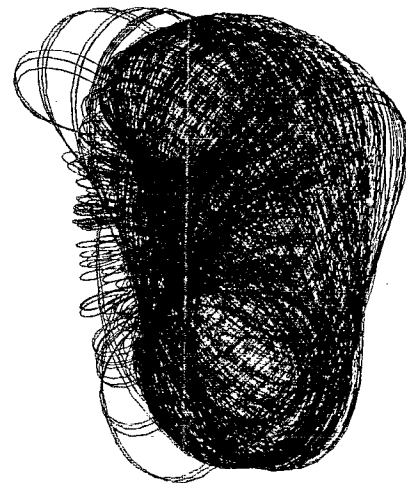
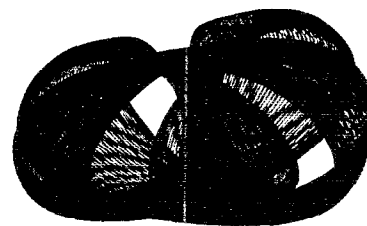


FIG. 13. Projections of phase-space trajectory in the  $v_1$ - $v_2$  plane for a particle starting from different initial locations with  $St = 2.4$  and  $\gamma = 0$ . All of these four attractors represent particle orbit in a period of 614 time units and have a same dimension of two.



(a).  $d_f = 3.18$



(b).  $d_f = 2.00$

FIG. 14. Two attractors of different dimensions observed for a particle starting from different initial locations with  $St = 1.0$  and  $\gamma = 0.85$ .

## V. CONCLUSIONS

A study of Lagrangian motion for a heavy particle requires direct numerical integration of the six-dimensional nonlinear system. We have provided, through numerical experiments, some preliminary qualitative and quantitative data about the nature of the solutions for the system. The particle trajectory is chaotic when the Stokes number is close to one and the drift is small. Periodic and quasiperiodic orbits are also observed for a variety of finite particle inertia and drift. The fractal dimension can be used to quantify the chaos. We found that the larger the fractal dimension, the more the attractor spreads on the Poincaré map. In general, the fractal dimension has a shape similar to the largest Lyapunov exponent. For most of the particle parameters, the fractal dimension and the Lyapunov exponents are independent of the initial location. However, multiattractors can exist.

The dispersion measure defined in this work is not related to the fractal dimension. We suggest that some direct measure of mixing based on line stretching<sup>15</sup> or return percentage for a forward–reverse diffusion process<sup>6</sup> be introduced. It might be possible to find a relationship between such direct measure and the fractal dimension. At present, direct quantitative measures of mixing for particles in steady flows are lacking. The fractal dimension might be more use-

ful to quantify the Lagrangian motion than the diffusivity, since, as seen in this work, the diffusivity cannot always be defined.

The quantification of chaotic dynamics shows that a Stokes number of one as well as a drift parameter close to one can be of physical significance. Structure bifurcation is observed when the drift parameter is close to one. Further work is needed to identify the nature of the bifurcations, the possibility of quasiperiodic orbits of higher dimension, and the effect of initial conditions for a range of  $St$  and  $\gamma$  values. It is to be borne in mind that our conclusions are specific to the single set of ABC flow parameters and limited sets of initial conditions considered.

#### ACKNOWLEDGMENTS

One of the authors (LPW) acknowledges the use of the computing facility at the Center for Fluid Mechanics, Turbulence, and Computation, Brown University during the critical time of the work. Part of the computation was done at the Pittsburgh Supercomputer Center. Suggestions and

support from Prof. Martin R. Maxey at Brown University are greatly appreciated as are the comments of the reviewers.

- <sup>1</sup> H. Aref, S. W. Jones, and O. M. Thomas, *Comput. Phys.* **2**, 22 (1988).
- <sup>2</sup> T. Dombre, U. Frisch, J. M. Greene, M. Hénon, A. Mehr, and A. M. Soward, *J. Fluid Mech.* **167**, 353 (1986).
- <sup>3</sup> H. Aref and S. Balachander, *Phys. Fluids* **29**, 3515 (1986).
- <sup>4</sup> J. Chaiken, C. K. Chu, M. Tabor, and Q. M. Tan, *Phys. Fluids* **30**, 687 (1987).
- <sup>5</sup> J. B. McLaughlin, *Phys. Fluids* **31**, 2544 (1988).
- <sup>6</sup> H. Aref and S. W. Jones, *Phys. Fluids A* **1**, 470 (1989).
- <sup>7</sup> L. P. Wang, T. D. Burton, and D. E. Stock, *Phys. Fluids A* **2**, 1305 (1990).
- <sup>8</sup> A. Crisanti, M. Falcioni, A. Provenzale, and A. Vulpiani, *Phys. Lett.* (in press).
- <sup>9</sup> J. Kaplan and J. Yorke, *Lecture Notes in Mathematics* (Springer-Verlag, New York, 1979), Vol. 730, p. 204.
- <sup>10</sup> A. Ralston and P. Rabinowitz, *A First Course in Numerical Analysis* (McGraw-Hill, New York, 1978), p. 194.
- <sup>11</sup> V. I. Oseledec, *Träns. Moscow Math. Soc.* **19**, 197 (1968).
- <sup>12</sup> S. N. Rasband, *Chaotic Dynamics of Nonlinear Systems* (Wiley, New York, 1990).
- <sup>13</sup> A. Wolf, J. B. Swift, H. L. Swinney, and J. A. Vastano, *Physica D* **16**, 285 (1985).
- <sup>14</sup> M. F. Doherty and J. M. Ottino, *Chem. Eng. Sci.* **43**, 139 (1988).
- <sup>15</sup> J. M. Ottino, *Annu. Rev. Fluid Mech.* **22**, 207 (1990).